Chemometry integrated add on studies of surface, thermogram and FT-Raman spectral datasets to deduce additive chelation potential of nutraceutical ligands

Authors: Sree varsha[*], K N Lokesh [a,*], Channarayappa [a, b], Marikunte Venkataranganna[c]

[a] Ramaiah Institute of Technology, Bengaluru-560054, Karnataka, India.
[b] Ramaiah College of Arts and Science, Bengaluru- 560054, Karnataka, India.
[c] Connexios Life Sciences Pvt Ltd Bengaluru- 560058, Karnataka, India.

[a ,b*] **Author for correspondence**

Department of Biotechnology, Ramaiah Institute of technology, Bengaluru-560054

Karnataka, India. ′

Abstract

Identification or discovery of novel heavy metal chelating antidotes demand extensive study of metal–ligand interactions *via* supramolecular co-ordination chemistry. Metal -ligand interaction studies are crucial in various clinical conditions ranging from cancer, endocrinological and neurological conditions. In the present investigation, we demonstrated the usefulness of integrating a chemometric approach with a prototype chelation study using nutraceutical bioactive ligands (curcumin, quercetin & gallic acid) with Fe(III). The formulated co-ordination complexes were analyzed using chemometric approaches such as, SEM integrated directionality analysis (SEM-DA), which provided an important lead to mark the topographical features of selected bioactive ligands and their respective coordination complexes. The analysis of the DSC thermogram by descriptive statistics confers unique heat signatures exhibited by bidentate and tris-bidentate Fe(III) coordination complexes, which were further substantiated by Box–Whisker plots. Furthermore, the FT-Raman spectral analysis with PCA provided additional statistical leads to confirm the unique features of bi-dentate and tris-bidentate coordination complexes. Thus, the present investigation substantiates that the integration of the chemometric approach with conventional analytical studies such as SEM, DSC, and FT-Raman provided crucial supplementary quantitative and statistically reliable data sets for structural characterization and elucidation of the additive denticity of selected ligands.

Key words: Nutraceuticals, chemometry, FT-Raman, Directionality analysis, iron chelation

Graphical Abstract

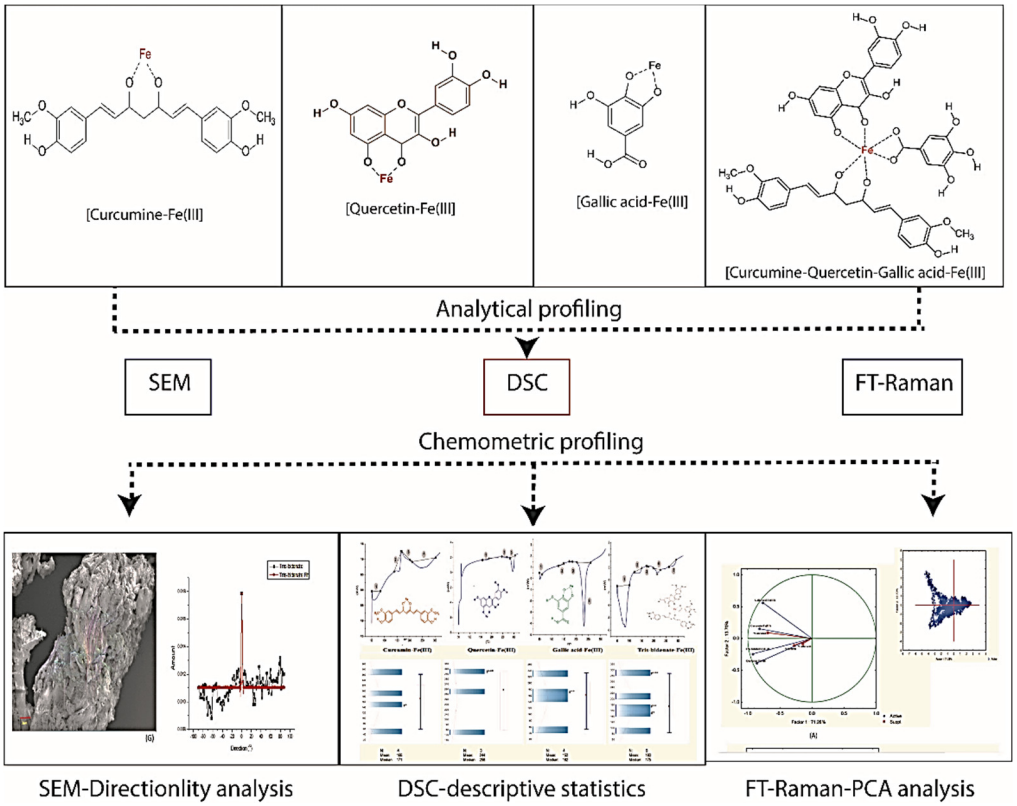

Introduction

Supramolecular coordination chemistry of bioactive ligands plays a pivotal role in the discovery, characterization, and standardization of new chemical entities (NCE's) & new molecular entities (NME's) of therapeutic interest, drug delivery systems and diagnostic agent, among others. Elevation of the concentration of essential and non-essential metal concentrations in the physiological system contributes to several clinical complications such as zinc, mercury poisoning, iron overload conditions and related neurological conditions. In such cases, supramolecular coordination chemical plays lead role in discovery and characterization of metal-chelating ligands or antidotes **(1-4).**

The efficiency of metal-chelating ligands assessed based on various parameters. The denticity is most important among them. The term denticity in coordination chemistry refers to the number of donor groups of a ligand(s) capable of binding centrally placed metal atoms in a coordination complex. Based on metal chelation ability, ligands are classified as mono-dentate, bi-dentate, tris-dentate, etc. The efficiency of metal-chelating ligands is expressed in terms of denticity profile, e.g., during the iron overload condition, the excess of iron in blood or plasma chelated by using standard intervention, namely desferrioxamine mesylate (DFO). It tends to form a hexadentate coordination complex with Fe(III) & subsequently subjected to clearance by physiological systems. Many natural bioactive ligands possess limited denticity (bidentate); thus, their metal chelation ability is incomparable to that of DFO and other therapeutic regime. However, several approaches have been reported to improve the denticity profile of natural bioactive to chelate Fe(III), such as using bioactive(s) as using additive or synergistic combination or derivatization of bioactive by using a specific linker, among others **(5-7)**.

In supramolecular coordination chemistry, the ligand and metal interaction elucidated by various analytical or hyphenated analytical techniques such as single-crystal X-ray crystallography, electron spray ionization-mass spectroscopy (ESI-MS), nuclear magnetic resonance (NMR), liquid-chromatography-Mass spectroscopy LC-MS, isothermal titration calorimetry, phase modulation fluorometry (PMF), circular dichroism spectroscopy (CDS), scanning probe microscopy (SPM), among others. Moreover, co-crystallization ligand(s)-metal interaction for in-vitro or ex-situ analysis do encounter various limitations **(8).**

The *in situ* or *ex-situ* analysis of therapeutic ligands-metal interaction study requires extensive preprocessing of biological samples followed by analytical or spectroscopic profiling. The processing of whole blood or serum is essential to avoid the interference of plasma protein or enzymes in the sample. The pre-treatment of the sample with nitric acid and hydrogen peroxide & subsequent heat digestion. Followed by resuspension of the sample into ultrapure water for further analysis. There are several cases studies to confer *in situ* or *ex-situ* characterization of ligand-metal complex. The ICP-OES or ICP-MS commonly performs the essential or non-essential trace elements profiling in blood or serum **(9)**. The "desferrioxamine-cheatable iron(III)" (DCI) in serum quantified in the form fluorescein-desferrioxamine (FI-DFO) probe followed by fluorometric analysis **(10).** The antibiotic norfloxacin-Fe(III) interaction in patient serum was determined via coupling of cloud point extraction procedure followed by UV-spectrophotometric analysis **(11).**

The chemometric uses the mathematical or statistical tool to analyze chemical data to retrieve statistically reliable information. There are several chemometric approaches has been reported to

characterize phytochemicals or herbal formulations *viz* classical least square (CLS), principal component analysis (PCA), window factor analysis (WFA), interative target transformation factor analysis (ITTFA) among others. The chemometric approach is used extensively to characterize the interaction between natural macromolecules with metal complexes of biological importance. Nanoparticle-metal adducts of therapeutical or diagnostic application are also characterized efficiently by using such approaches. The chemometric approach also helps to elucidate chemo-biological interaction of physiological significance **(12-14).**

With the help of the present investigation, we tried to exemplify the importance of integrating the chemometric approach with conventional analytical studies such as SEM, DSC, and FT-Raman spectroscopy to retrieve supplementary information to substantiate structural & chemical characteristics of coordination complexes. We selected a standardized combination of bioactive curcumin, quercetin & gallic acid **(5, 15)**. Further, the respective bi-dentate-Fe(III) & tris-bidenate coordination complexes were characterized by adopting the following approaches: i) Topography analysis of scanning electron microscope (SEM) image(s) by directionality analysis (SEM-DA), ii) DSC thermogram analysis by descriptive statistics iii) FT-Raman spectral analysis by principal component analysis, in order to substantiate proof of concept and iv) In -vivo proof of concept to deduce the additive nutraceutical in iron(III) dextran intoxicated murine models.

Materials and Methods

Chemical & materials

Generic bioactive ligands such as curcumin, quercetin & gallic acid (Sigma-Aldrich Co., St. Louis, MO, USA), ferric chloride (S.D. Fine, Chemicals Mumbai, India), and methanol (HiMedia, Mumbai, India) were purchased and stored under specified conditions.

The chemometric analysis analytical datasets was performed by adopting following steps. Step-1: Formulation or preparation of stochiometric combination of nutraceutical(s)-Fe(III) coordination complexes. Step-2: Scanning electron microscopy & directionality analysis (SEM-DA). Step-3: Differential scanning calorimetry (DSC) & descriptive statistics (DSC-DS). Step-4: FT Raman spectroscopy & PCA analysis, and; Step-5: In-vivo validation in iron(III) intoxication murine model.

Preparation of coordination complexes of bioactive ligands with iron(III)

The bidentate coordination complexes of curcumin-Fe(III), quercetin-Fe(III), and gallic acid-Fe(III) were prepared by refluxing the pre-standardized molar ratio of bioactive ligands with Fe(III), which were taken in the ratio of 3:1 in methanol separately. The mixture was refluxed at 60°C for about 1h under controlled condition. The mixture was concentrated and filtered. The tris-bidentate coordination complex of [curcumin + quercetin + gallic acid- Fe(III)] was prepared by

refluxing 3 molar part of bioactive ligands comprised of 1 mole each of curcumin, quercetin, and gallic acid with 1 mole of Fe(III)**.** Once the mixture refluxed, the contents were processed as that of bi-dentate coordination complexes. The bi-dentate curcumin-Fe(III), quercetin-Fe(III) and gallic acid-Fe(III) and tris-bidentate coordination-Fe(III) coordination complexes as shown in Scheme A,B,C&D respectively were subjected to analytical/spectroscopic studies followed chemometric analysis.

Scanning electron microscopy & directionality analysis (SEM-DA)

The bioactive ligand(s) and their respective Fe(III) coordination complex microstructure features were analyzed using SEM analyzer ZEISS ULTRA®55 (Carl Zeiss NTS GmbH, Oberkochen, Germany). The ULTRA 55 equipped with fully integrated energy and angle selective backscattered electron (EsB) and an Everhart–Thornley SE detector. It is coupled with a filtering grid maintained at a voltage of 0 – 1500 V, which enhances image quality, less adjustment for image acquisition, and sensitivity towards edge contrast & charging effect. Large multi-port analytical chamber equipped with fully motorized 5 axes eucentric stage offer enhanced analytical capabilities. The samples were subjected to sputtering prior to SEM analysis. Quantity sufficient samples applied onto the sample holder attached with double-sided carbon conductive adhesive tape (Agar Scientific, Stansted, UK). The field-emission operates at 0.1-30kV, and the SEM image recorded under low voltage (0.1-5kV). The opensource Fiji developed & released under GNU Public License was used to analyze the directionality analysis of the input or acquired SEM image **(16).** It analyzes the input image based on Fourier components, revealing the Gaussian distribution, discrete Fourier function, and orientation map of the input image (17). The directionality analysis generates an orientation map for the input image and results in the generation-colored orientation map (18).

Differential scanning calorimetry (DSC) & descriptive statistics (DSC-DS)

The DSC profile of curcumin, gallic acid, and quercetin & their respective bi-dentate and tris bi-dentate-Fe(III) coordination subjected to comparative thermal behavior study. The DSC thermogram was recorded in a DSC1 STAR system (Mettler-Toledo AG, Analytical CH-8603 Schwerzenbach, Switzerland). The samples heated at rate of 5˚C /min in the temperature range of 20˚C - 350˚C. The thermogram's dynamic measurement was carried out with dry nitrogen maintained at a flow rate of 50 ± 4 ml/min. The thermogram obtained from DSC was processed by Statistica 13, which has generated descriptive statistics and the frequency of distribution (19).

FT Raman spectroscopy & PCA analysis

The Raman spectra of bioactive ligands and their respective Fe(III) coordination complex were characterized by FT Raman spectroscopy HR 800 (Horiba Scientific). Samples exposed to internal excitation laser (He-Ne), equipped with a laser excitation wavelength of 663 nm; 600 grooves/mm grating, laser energy adjusted to 3-25 mW. The Horib 800 system operated in confocal mode with spatial resolution up 1 µm. FT Raman HR 800 integrated with Olympus BX41 with objectives of 10X (NA 0.25), 50X (NA 0.75), 50X (NA 0.5), 100X (NA 0.9) coupled with Peltier-cooled CCD 1024 X 256 px detector system. PCA is a powerful statistical tool for efficient data evaluation and interpretation, graphically representing the correlation between the variables and bringing down the dataset's multidimensional facets. The multivariant exploratory technique by PCA tool of

STATISTICA 13.2 (Tibco Inc) was used to perform spectral data analysis. The principal component analysis (PCA) is a powerful multivariate statistical method that used data reconstruction and data sorting. PCA generates a new set of orthogonal axis or variables known as principal components (PC). PC's data sets express total variability across the provided data sets to find correlated and uncorrelated parameters. Each principal component defined by a correlation matrix associated with a vector known as an eigenvalue. The eigenvector used to express the variance among the major PCs. The correlation matrix used to calculate the loading score of the corresponding PCs computed by using the following expression (1)

$$PC = a_1\left(\frac{x_1 - \bar{x}_1}{SD_1}\right) + \cdots \qquad (1)$$

Where a_1: loading score of a linear transformation, x_1: values correspond to the original variable, $\bar{x}_1$: mean value of the corresponding variable, SD_1: standard deviation (20).

Variance reduction or data discrimination was visualized by using biplots of PCs which depicted the identity of the correlation variable (21).

Result & Discussion

The bioactive ligands curcumin, quercetin & gallic acid, and their respective bidentate / tris-bidentate Fe(III) coordination complex analytical profile (SEM, DSC & FT-Raman) characterized using a chemometric approach to obtain statistically reliable datasets for comparative analysis.

SEM-directionality analysis (SEM-DA)

The SEM is commonly used to analyze the surface topography and related features of a wide range of substances. In the present investigation, the SEM image of bioactive ligands and their respective coordination complexes were further analyzed by the directionality analysis (DA) tool, as shown in **Fig.1(A-G).** The DA provides insight into the structural orientation map of bioactive ligand(s) and their respective coordination complexes analyzed in terms of Fourier Gaussian function, which provides quantitative datasets such as spline direction (°), dispersion (°), amount, and goodness of fit (R^2), as shown in **Table.1**. The surface topography of acquired SEM image mapped with DA which possesses a low quantitative score for tis-bidentate coordination of [curcumin + quercetin +gallic - Fe(III)] reported as spline direction (°) =0.06, dispersion (°) =0.82, amount=0.02, and goodness of Fit (R^2) = 0.39 as compared to their bidentate and individual counterparts as shown in **Table 1.** Low DAT score, possibly due to the tris-bidentate coordination possesses high steric hindrance on formed supramolecular coordination compound **(22)**

Dynamic differential scanning calorimetry

The thermal analysis of bioactive ligands-Fe(III) coordination complex(s) had possessed unique thermal signatures measured as endothermic peaks. The resulting endothermic peaks from the bidentate and tris bidentate- Fe(III) coordination complexes were closely analyzed, and the inference was made using descriptive statistics. The selected bioactive ligands such as curcumin, quercetin & gallic acid, and their respective Fe(III) coordination complex exhibited unique thermal peaks, as shown in **Fig. 2.** It possesses several endothermic peaks and glass transition phase (T_g). Further consolidated analysis of the thermogram in terms of T_{onset}(°C), T_{peak} (°C), T_{endset} (°C) & ΔH provided crucial leads for interpretation as summarized in **Table.2.** Comparative analysis of DSC analysis has revealed that the thermogram of tris-bidentate co-ordination complex [curcumin-

quercetin-gallic acid-Fe(III)] closely corresponds to individual thermograms possessed by of bidentate coordination complexes i.e., [curcumin- Fe(III)], [quercetin -Fe(III)] & of [gallic acid-Fe(III)]. The descriptive statistical analysis was integrated with DSC thermograms to substantiate this finding, as shown in **Fig. 2.**

Bidentate [curcumin- Fe(III)] coordination complex results in 4 endothermic peaks (N=4), bidentate [quercetin -Fe(III)] results in 3 endothermic peaks(N=3) & bidentate[gallic acid-Fe(III)] results in 4 endothermic peaks (N=4). Whereas tris-bidentate [curcumin-quercetin-gallic acid-Fe(III)] resulted in 5 (N=5) endothermic peaks. Integration of descriptive statistics with the DSC profile provides comparable and statistically reliable data sets. The frequency distribution bar was marked with special characters such as $\#^{*}$, $\#^{**}$, $\#^{***}$, which helped in the easier correlation of frequency distribution bars of bidentate and trisbidenate coordination complexes of the bioactive ligands. The endotherm-2 (N-2) of tris-bidentate corresponds to endotherm-2 (N-2) of [curcumin-Fe(III)] indicated as ($\#^{*}$).The endotherm-5 (N-5) of trisbidenate coordination complex corresponds to endotherm-3 (N-3) of [quercetin -Fe(III)], marked as ($\#^{***}$).Whereas, the glass transition phase (T_g) of the trisbidenate coordination complex (N-3) correlates to The glass transition phase (T_g) of [gallic acid-Fe(III)](N-3) indicated by ($\#^{**}$).The endotherm profile of tris-bidentate-Fe(III) and their corresponding bidentate coordination-Fe(III) complex endotherms are well distributed within the Box-whisper plot with distinct highest-lowest observation, upper-lower quartile & interquartile ranges as shown in **Fig.2.**

DSC thermogram analysis further provided an important lead on polymorphic transition (solid-solid). The chelation of bioactive ligand(s) with Fe(III) results in typical $\alpha \rightarrow \beta$ solid-solid transition and few λ transitions observed due to weak ferromagnetic property. Typically, the $\alpha \rightarrow \beta$ solid-solid transition initiates from low temperature (α) & end as high temperature (β) endothermic peaks. The β-form gives rise to different shape peaks, depending on the sample size, nucleation rate, etc. The chelation of curcumin with iron(III) exhibits different polymorphic transition $\alpha \rightarrow \beta$ transition without any λ transition. The lambda solid-solid transition (λ) is typically V-shaped and extremely weak; generally, materials that possess the ferromagnetic property at low temperature lose their magnetic property and possess non-ferromagnetic property above the curie point. This phenomenon exhibited by bidentate quercetin and gallic acid. Quercetin shows curie point at endotherm-1 and gallic exhibits curie point at endotherm-3 as shown in Fig.**2**. The tris-bidentate bioactive ligand(s)-Fe(III) complex exhibits $\alpha \rightarrow \beta$ transition observed as endotherm-1, this kind of transition which may occur due to a small number of larger crystals present in the coordination complex. It also produced bizarre shape peaks along with β & λ transitions, as shown in **Fig.2.** Interestingly it shares the endotherm regions that share the thermogram heat signatures of corresponding bidentate- Fe(III) complexes, as shown in **Table.1**. DSC usually detects the phase transition in the molecular structures, which exhibits unique heat flux gradients at varying temperatures. The phase transition is associated with the eutectic and non-eutectic transition, which can be observed with DSC profile of the coordination complexes **(23).** The descriptive statistic aided analysis of the DSC profile of the bioactive ligands and their respective bidentate and tris-bidentate coordination complex provided comparative statistically valid datasets for a comparative analysis.

FT-Raman Analysis

FT-Raman analysis of bi-dentate-Fe(III) and tris-bidentate-Fe(III) used to compare their structural features and to deduce the role of functional groups that are involved in the formation of dentate

coordination with Fe(III).Curcumin exhibits distinct peaks of ν(C=O) & ν(C-OH) at 1631 cm^{-1} & 1419 cm^{-1} respectively. Chelation of curcumin with Fe(III) results in the reduced intensity of ν(C=O) & ν(C-OH), followed by peak shift recorded at1628 cm^{-1}& the suppression of ν(C-CH) & ν(C-O) at 1308 cm^{-1} & 1236 cm^{-1} respectively. This indicates a phenolic functional group (-OH) of curcumin is actively involved in forming a bidentate coordination complex with Fe(III). Further transformation of the aromatic ring due to polymorphism was also detected as ν(C-C_{ring}) of curcumin at 1596 cm^{-1}, which is suppressed drastically in bidentate curcumin-Fe(III) coordination complex with declined %T, which falls in the range of 150 to 400 %T**,** as shown in **Fig.3 (A).** Quercetin possesses distinct functional groups such as weak ν(C=O) at 1686 cm^{-1}, aromatic (C-C)$_{ring}$ at 1636 cm^{-1}, phenol function group (-OH) at 1433 cm^{-1}, C-OH $_{(Bending)}$ at 1347 cm^{-1} weak OH def vibration at 1232 cm^{-1} and aromatic CH def vibration at 1129 cm^{-1} without any distinct D and G bands. The chelation of quercetin with iron(III) results in complete suppression of ν(C=O) and peak shift of aromatic (C-C) $_{ring}$. The splitting of the band at 1433 cm^{-1} due to -OH & C=O attached at C_3 & C_4 position respectively, are vanished or attenuated due to coordinate complex formation with iron(III), indicating the involvement -OH & C=O in the formation of a bidentate coordination complex with iron(III) as shown in **Fig. 3(B)**. In the case of gallic acid, the aromatic ring stretching vibrations (C-C) exhibit a sharp peak at 1507 cm^{-1}, whereas carboxylic group ν(C=O) show a prominent vibration band at 1613 cm^{-1}. The hydroxyl mode ν(-OH) of the carboxylic acid of gallic acid have possessed two bands at 1347 cm^{-1} and 1246 cm^{-1}. The bidentate gallic acid-Fe(III) coordination complex possesses prominent suppression of ν(C-C) aromatic ring along with ν(-OH) of carboxylic acid, which infers that the -OH functional groups play an important role in the formation of a coordination complex, as shown in **Fig.3(C).** Tris-bidentate complex exhibited C-O-C stretching at 1641 cm^{-1}, (C-C) $_{ring}$ 1531 cm^{-1} of curcumin-Fe(III) bidentate coordination complex. The Residual aromatic -CH def vibration at 1002 cm^{-1}, residual -OH def vibration at 846 cm^{-1} of gallic acid. Whereas, D and G bands of quercetin-Fe(III) at 605 cm^{-1} and 539 cm^{-1}, respectively, The Fe(III)-O system of tris-bidentate coordination complex was observed at a range of 86 cm^{-1} to 442 cm^{-1} as shown in **Fig.3(D).**

IR and Raman spectroscopy are the most used vibrational spectroscopic technique used to assess molecular motion and compare functional group fingerprints in molecular species for comparative analysis. In the present investigation, Raman spectroscopy preferred to characterize bioactive ligand(s)-Fe(III) coordination complex due to the following reasons (a) Raman and IR differ from each other based on the type of molecular transition that is taking place. The molecular transition is regarded as Raman active when changes in the polarizability of molecules during vibration occur due to positional changes in the electron cloud (b) IR detects molecular transition in the dipole moment during vibration. A molecule with strong dipole movement is hard to polarize (c) IR spectra record and show irregularity in absorbance or transmittance. In contrast, Raman spectra exhibit elastic scattering of light (Rayleigh) and two equal distance lines of strokes and anti-stroke, enhancing the resolution of spectra with weak signals (d). FT-Raman has increased light stability from the laser source. Sensitive amplification of weak signal due to ultrasensitive detectors, which are sometimes may not be detected by IR spectroscopy. Raman spectroscopy is one of the most sensitive methods to characterize disorder in the molecules that possess sp^2 hybridization or further series of hybridization **(24, 25).** Typically, the D&G and bands correspond to disorder in molecular structure as a result of sp^2d^2 hybridization of carbon while the formation of coordination complex formation with transitional metals. The observed splitting in the D and G band is due to a localized vibrational mode of impurities, i.e., Fe(III), resulting in observed splitting. The distinct sp^3d^2 hybridization and Fe(III)-O in tris-bidentate-Fe(III) coordination complex may contribute to

stearic strain on the supramolecular structure resulting in a distinct decline in the %T in resulted coordination complexes. **Table No.3** exhibits the significant PCs generated from FT-Raman spectral input of bioactive ligands (supplementary) and their respective coordination complexes (active). The first principal component (PC1) possesses the highest eigenvalue of 2.85 that accounts for 71.28% of variability among the tested data sets. The subsequent PCs i.e., PC2, PC3 and PC4 had eigenvalues of 0.54, 0.44 & 0.15 which accounts for 13.70%, 11.18% & 13.14% of total variance in the provided datasets respectively. The eigenvalue >1.0 is regarded as a significant descriptor for the detection of data variance. The PC1 describes 71.25% of the total variance among provided datasets and their corresponding loading scores. Interestingly the correlation matrix indicates maximum contribution of loading score for tris-bidentate-Fe(III) (-0.92) followed by bidentate Fe(III) coordination complexes such as quercetin-Fe(III) (-0.86); curcumin-Fe(III) (-0.82), gallic acid-Fe(III)(-0.76). The unchelated form of supplementary bioactive exhibits the least loading score as compared to their respective coordination complexes, as shown in **Table no 3.** The biplots visualize the position of input variables in two-dimensional space. Variables that are close to each other and farther from the origin are positively correlated. In contrast, the variables that are positioned opposite to one another are negatively correlated. The curcumin and its corresponding Fe(III) coordination complex exhibit a positive correlation. Quercetin, gallic acid, and corresponding coordination complexes are negatively correlated, as shown in **Fig.4(A).** The nonlinear interactive partial least square (NIPALS) integrated PCA analysis is used profoundly in statistics for multivariant data analysis. The Hotelling T^2 control chart was used to detect the fault in provided FT-Raman spectra. In the present investigation, the cases that crossed the controlled Hotelling T^2 mark of 23.501 are regarded as out-of-control cases. To detect variables that influence those points or cases for crossing out-of-control mark in Hotelling T^2. Interestingly, the unchelated form of bioactive ligands such as curcumin, quercetin, and gallic acid possesses the highest cases for outliers as compared to their respective Fe(III) coordination complex show in **Fig. 5(A). The** influential variable identified by decomposed T^2 analysis as shown in Fig.5(B). The outcomes further substantiated by contribution plo**t Fig.5(C),** which concludes that the tris-bidentate Fe(III) coordination complex possesses a maximum PCA score contribution score compared to the corresponding bidentate and individual bioactive ligands, as shown in **Fig. 5(B).**

CONCLUSION

Discovery of novel heavy metal chelating antidote demands extensive exploration of metal-ligand co-ordination complexes. Which needs extensive pre-processing from in-situ samples followed by hyphenated analytical studies. With the help of the present investigation, we tried to exemplify that integrating the chemometric approach with conventional surface analytical/ spectroscopic studies will be helpful to get supplementary statistically reliable datasets for characterization of bioactive(s)-metal coordination complexes which were validated by In-vivo studies. Such prototype studies provides platform to retrieve useful information from analytical dataset by chemometric approach for discovery of new chemical entities(NCEs) or new molecular entities (NMEs) with greater reliability, time bound and cost effective manner.

Acknowledgement

Author would like to convey gratitude to research centre of Ramaiah Institute of Technology Bengaluru & Connexios Life sciences Pvt. Ltd Bengaluru for providing research facilities. Analytical facilities were provided by Society for Innovation and Development centre (SID) & Centre for Nano-science- Engineering, Indian institute of Sciences (IISc) Bengaluru.

Conflict of Interest

We hereby declare no conflict of interest.

REFERENCES

1. Casini A, Woods B, Wenzel M. The Promise of Self-Assembled 3D Supramolecular Coordination Complexes for Biomedical Applications. Inorg Chem. 2017;56(24):14715-29.
2. Li B, He T, Shen X, Tang D, Yin S. Fluorescent supramolecular polymers with aggregation induced emission properties. Polymer Chemistry. 2019;10(7):796-818.
3. Li Z, Song N, Yang Y-W. Stimuli-Responsive Drug-Delivery Systems Based on Supramolecular Nanovalves. Matter. 2019;1(2):345-68.
4. Zhou J, Yu G, Huang F. Supramolecular chemotherapy based on host-guest molecular recognition: a novel strategy in the battle against cancer with a bright future. Chem Soc Rev. 2017;46(22):7021-53.
5. Lokesh KN, Venkataranganna M, Raj GG, Patil H, Dave H. Augmentation of antioxidant and iron (III) chelation properties of tertiary mixture of bioactive ligands. Journal of Trace Elements in Medicine and Biology. 2018;45:114-24.
6. Zahrani NAAL, El-Shishtawy RM, Asiri AM. Recent developments of gallic acid derivatives and their hybrids in medicinal chemistry: A review. European journal of medicinal chemistry. 2020:112609.
7. Nobre CB, Sousa EO, Camilo CJ, Machado JF, Silva JMFL, Jaime Filho R, et al. Antioxidative effect and phytochemical profile of natural products from the fruits of “babaçu”(Orbignia speciose) and “buriti”(Mauritia flexuosa). Food and Chemical Toxicology. 2018;121:423-9.
8. Schalley CA. Analytical methods in supramolecular chemistry: John Wiley & Sons; 2012.
9. Laur N, Kinscherf R, Pomytkin K, Kaiser L, Knes O, Deigner H-P. ICP-MS trace element analysis in serum and whole blood. PloS one. 2020;15(5):e0233357.
10. Breuer W, Ermers MJ, Pootrakul P, Abramov A, Hershko C, Cabantchik ZI. Desferrioxamine-chelatable iron (DCI), a component of serum non-transferrin-bound iron (NTBI) used for assessing iron chelation therapy. Transfusion science. 2000;23(3):241-2.
11. Khammas ZA, Mubdir NS. Cloud Point Extraction Spectrophotometric Method for Mutual Determination of Norfloxacin and Iron (III) in Human Serum and Drug Formulations”, Chem. Sci. Transactions. 2015;4(2):483-97.
12. Kumar N, Bansal A, Sarma GS, Rawal RK. Chemometrics tools used in analytical chemistry: An overview. Talanta. 2014;123:186-99.
13. Berto S, Alladio E. Application of Chemometrics Tools to the Study of the Fe (III)–Tannic Acid Interaction. Frontiers in Chemistry. 2020;8:1172.
14. Jalalvand AR. Chemometrics in investigation of small molecule-biomacromolecule interactions: A review. International Journal of Biological Macromolecules. 2021.
15. Lokesh KN, Venkatarangana M. Exemplified screening standardization of potent antioxidant nutraceuticals by principles of design of experiments. Journal of Functional Foods. 2015;17:260-70.
16. Schindelin J, Arganda-Carreras I, Frise E, Kaynig V, Longair M, Pietzsch T, et al. Fiji: an open-source platform for biological-image analysis. Nat Methods. 2012;9(7):676-82.
17. Liu Z-Q. Scale space approach to directional analysis of images. Applied optics. 1991;30(11):1369-73.

18. Press WH, Teukolsky SA, Vetterling WT, Flannery BP. Numerical recipes in C++. The art of scientific computing. 1992;2:1002.
19. Kunze M, Jeong S, Paillard E, Winter M, Passerini S. Melting behavior of pyrrolidinium-based ionic liquids and their binary mixtures. The Journal of Physical Chemistry C. 2010;114(28):12364-9.
20. Shin E-C, Hwang CE, Lee BW, Kim HT, Ko JM, Baek IY, et al. Chemometric approach to fatty acid profiles in soybean cultivars by principal component analysis (PCA). Preventive nutrition and food science. 2012;17(3):184.
21. Yildiz E, Pinar H, Uzun A, Yaman M, Sumbul A, Ercisli S. Identification of genetic diversity among Juglans regia L. genotypes using molecular, morphological, and fatty acid data. Genetic Resources and Crop Evolution. 2021;68:1425-37.
22. Ren Y-P, Kong X-J, Hu X-Y, Sun M, Long L-S, Huang R-B, et al. Influence of Steric Hindrance of Organic Ligand on the Structure of Keggin-Based Coordination Polymer. Inorganic Chemistry. 2006;45(10):4016-23.
23. Diarce G, Quant L, Campos-Celador Á, Sala JM, García-Romero A. Determination of the phase diagram and main thermophysical properties of the erythritol–urea eutectic mixture for its use as a phase change material. Solar Energy Materials and Solar Cells. 2016;157:894-906.
24. Yan B, Gremlich H-U, Moss S, Coppola GM, Sun Q, Liu L. A Comparison of Various FTIR and FT Raman Methods: Applications in the Reaction Optimization Stage of Combinatorial Chemistry. Journal of Combinatorial Chemistry. 1999;1(1):46-54.
25. Vankeirsbilck T, Vercauteren A, Baeyens W, Van der Weken G, Verpoort F, Vergote G, et al. Applications of Raman spectroscopy in pharmaceutical analysis. TrAC Trends in Analytical Chemistry. 2002;21(12):869-77.

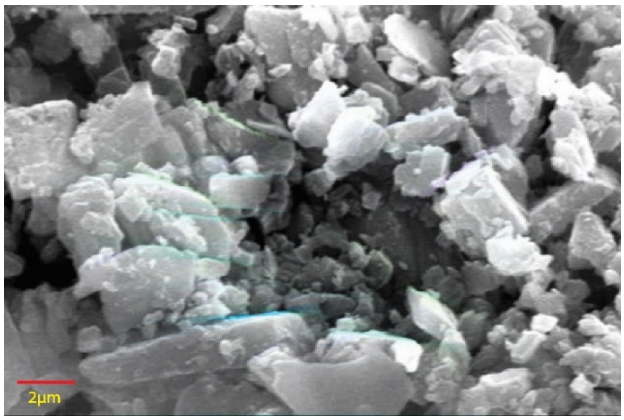

Fig.1 (A)

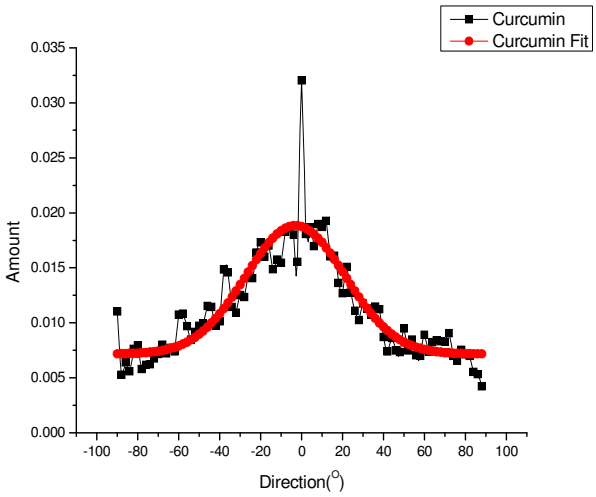

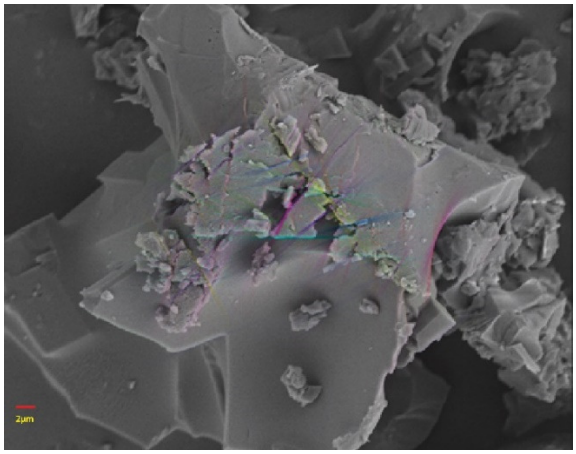

Fig.1 (B)

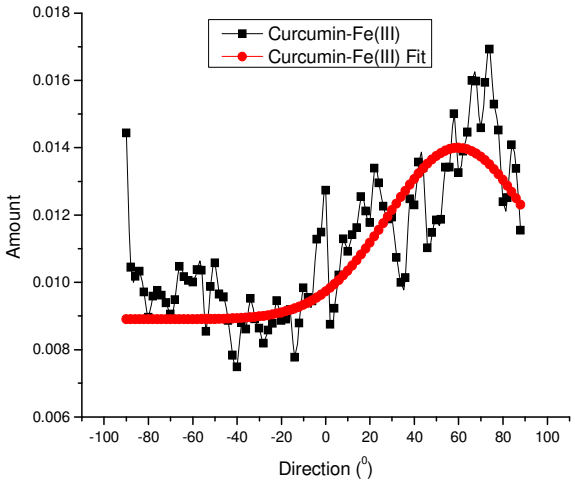

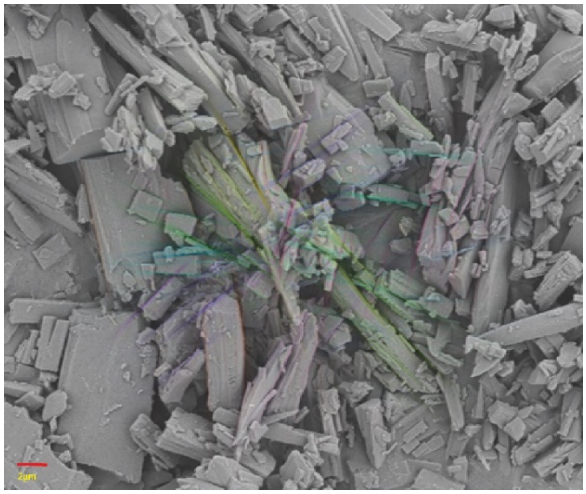

Fig.1 (C)

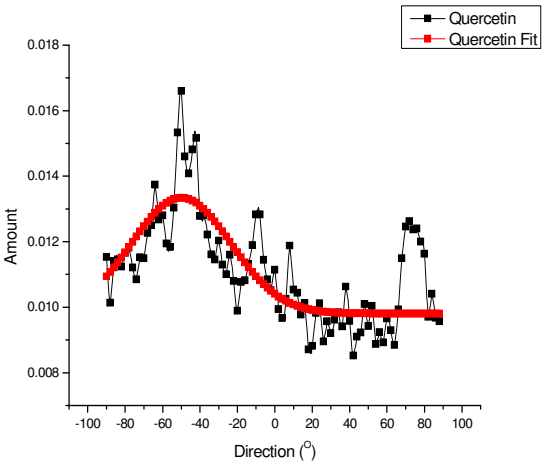

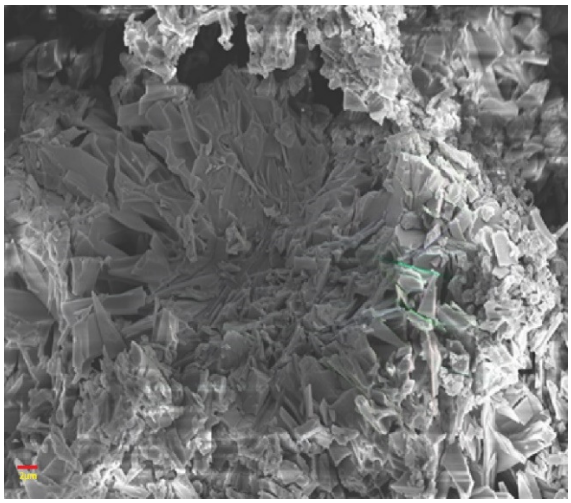

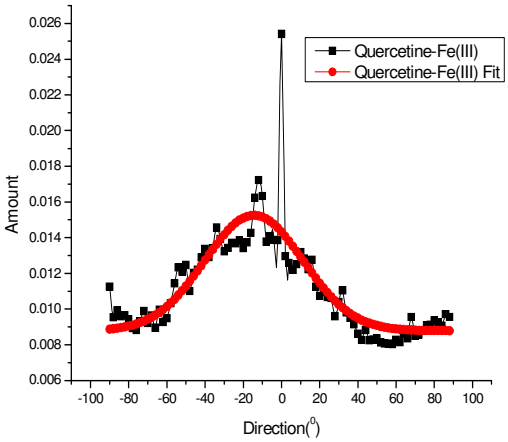

Fig.1 (D)

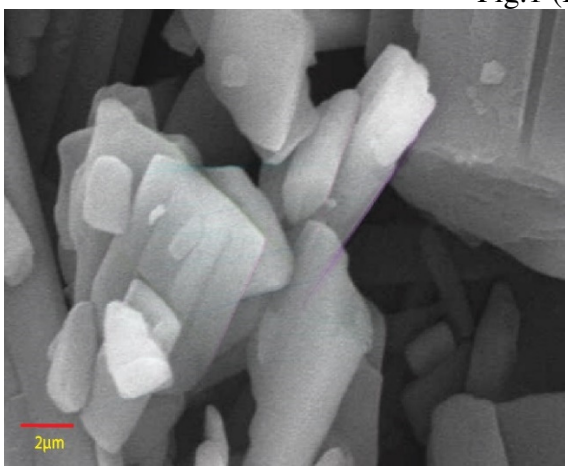

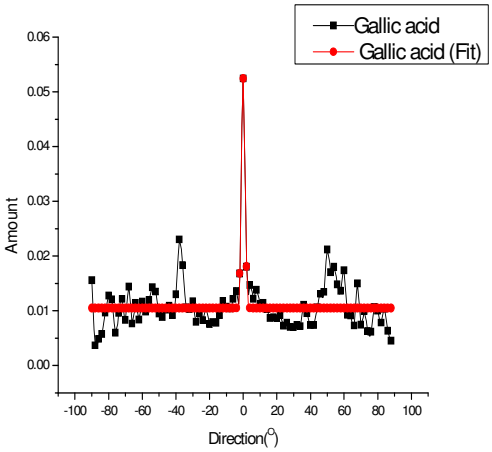

Fig.1 (E)

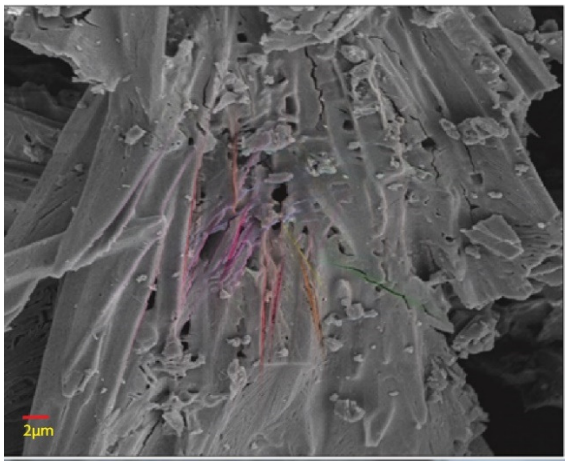

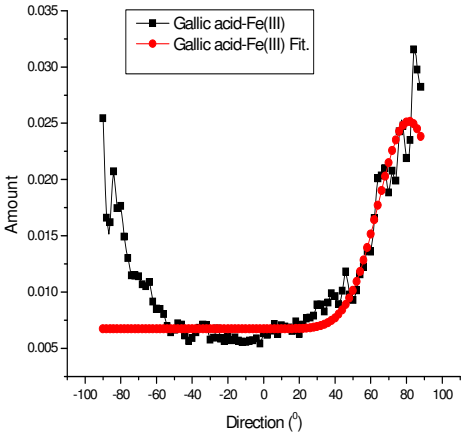

Fig.1 (F)

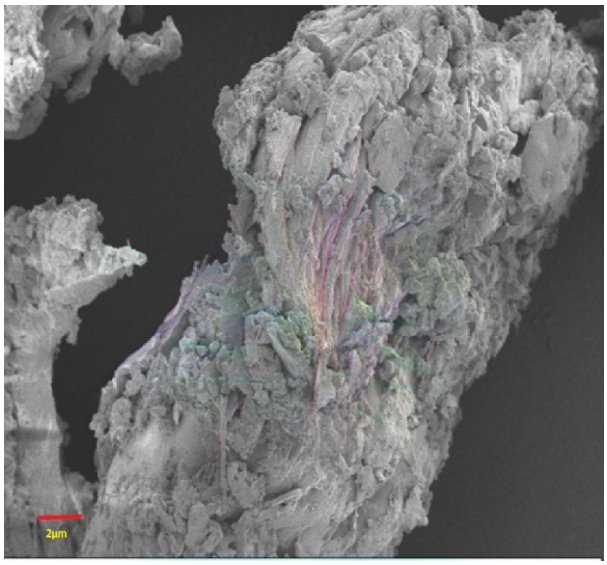

(G)

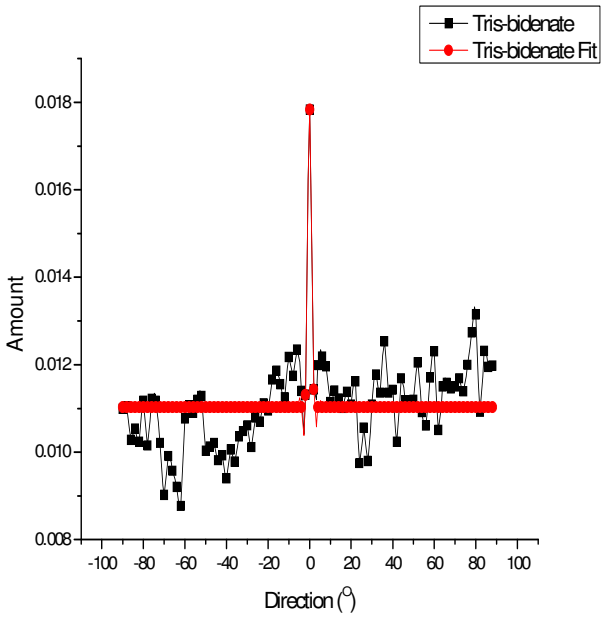

Fig.1 **(G)**

Fig. 1(A-G): SEM images along with directionality analysis profile of selected bioactive ligands and their respective Fe(III) co-ordination complexes **(A)** Curcumin; (B) Bidentate curcumin-Fe(III); (C) Quercetin; **(E)** Bidentate quercetin-Fe(III) (D) Gallic acid;**(F)** Bidentate gallic acid-Fe(III); **(G)** Tris bidentate curcumin-quercetin-gallic acid- Fe(III).

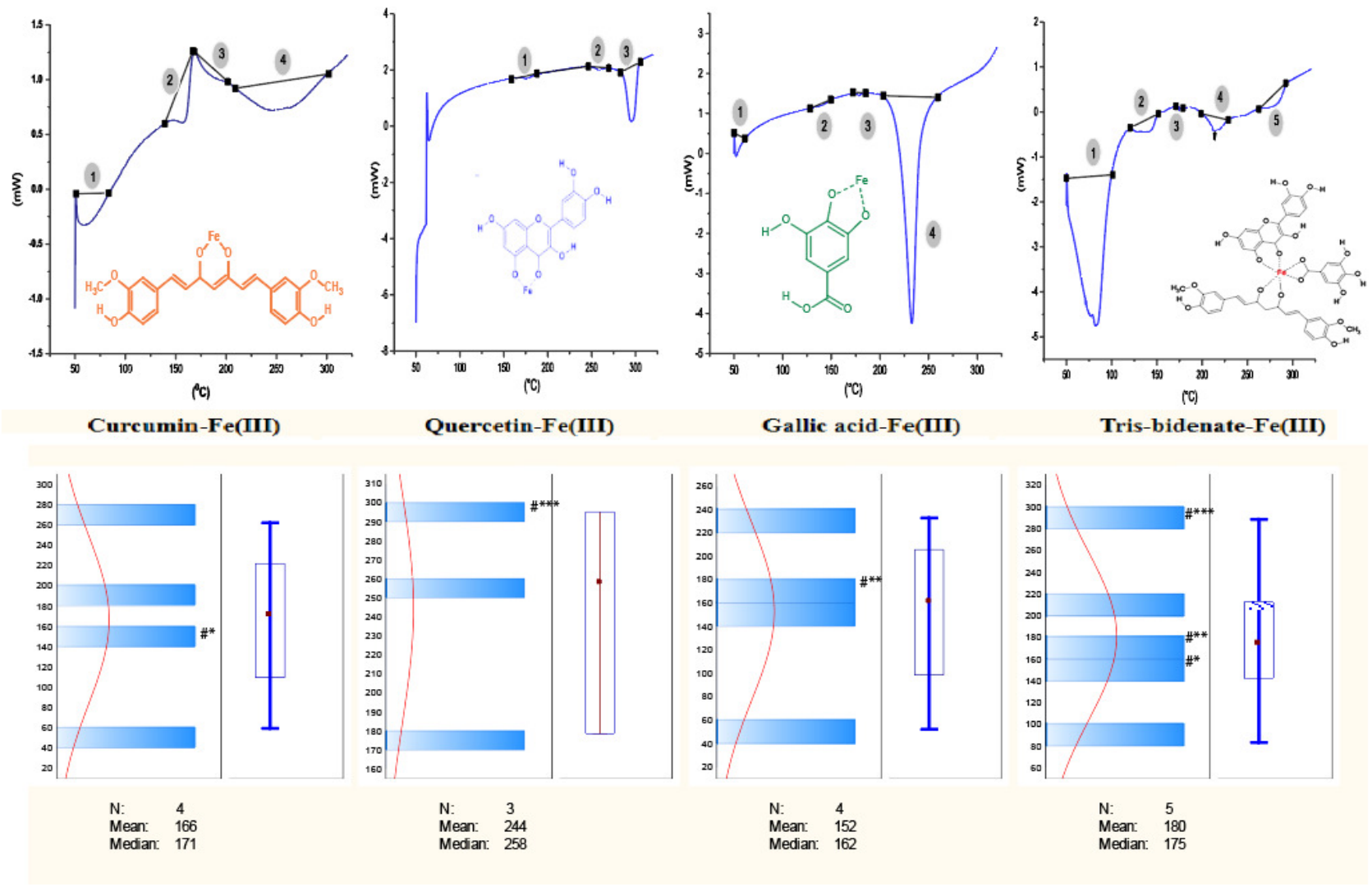

Fig. 2. Descriptive statistical analysis of DSC thermograph with help of Box & whisker plots depicting the comparative thermal analysis of bioaction ligands-Fe(III) co-ordination complexes.

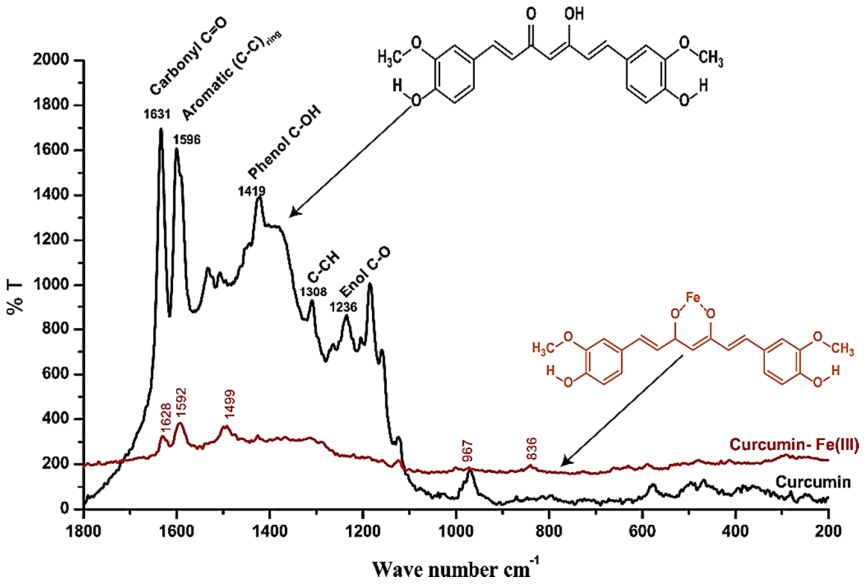
Carbonyl C=O
Aromatic (C-C)ring
1631
1596
Phenol C-OH
1419
C-CH
1308
Enol C-O
1236
1628
1592
1499
967
836
Curcumin- Fe(III)
Curcumin
% T
Wave number cm-1

3 (A)

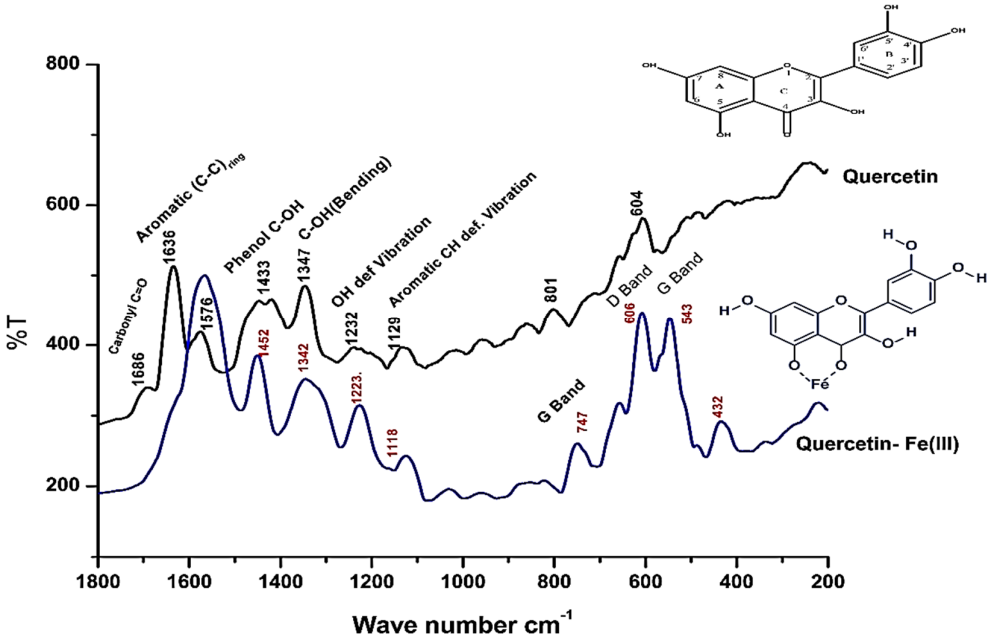
Aromatic (C-C)ring
Carbonyl C=O
1686
1636
1576
Phenol C-OH
1433
1452
C-OH(Bending)
1347
1342
OH def Vibration
1232
1223.
Aromatic CH def. Vibration
1129
1118
801
604
606
543
432
747
D Band
G Band
G Band
Quercetin
Quercetin- Fe(III)
%T
Wave number cm-1

3 (B)

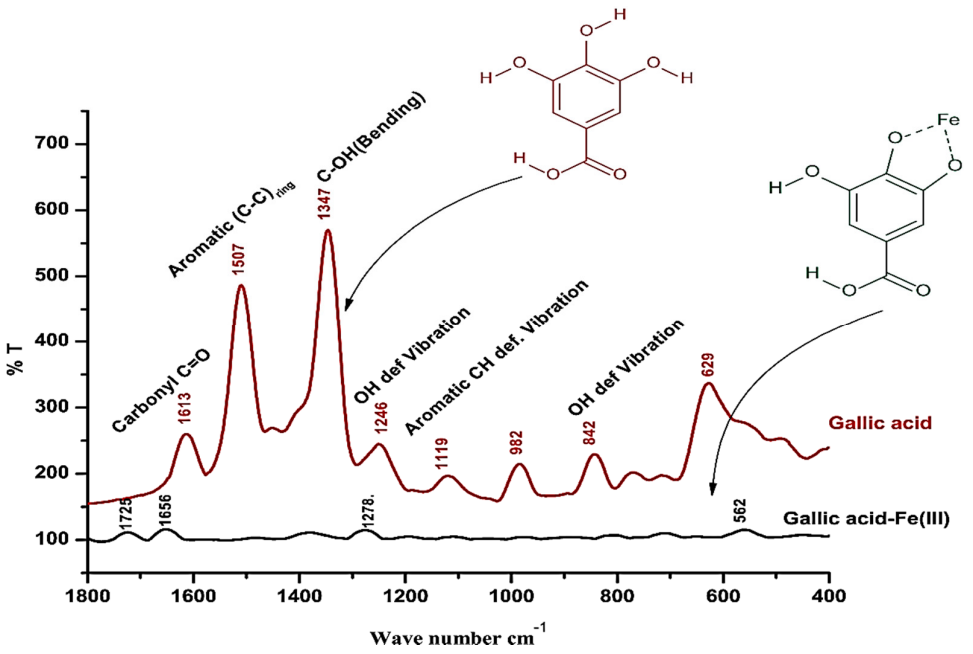

3(C)

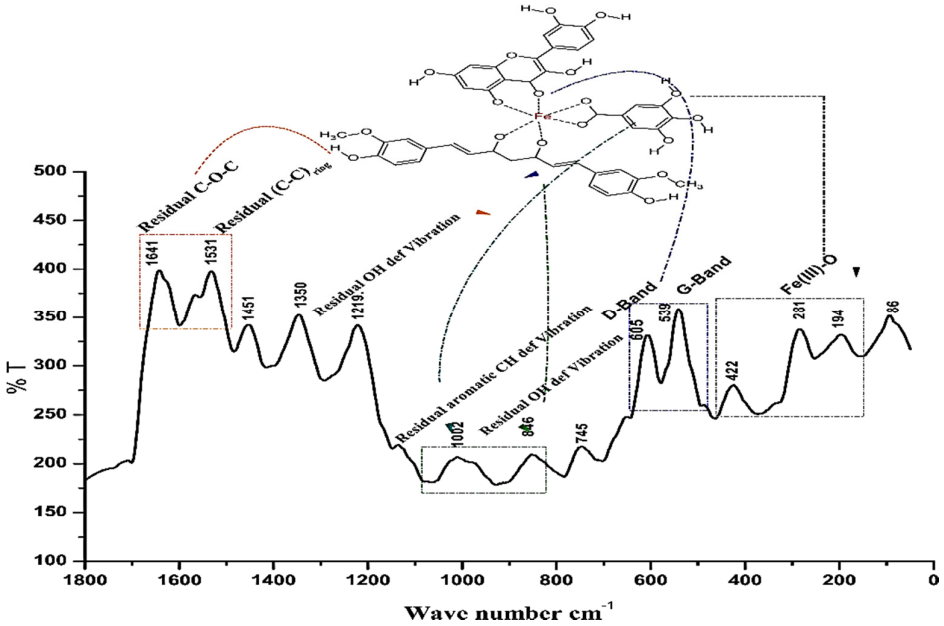

3 (D)

Fig. 3(A-D): FT-Raman spectra of bioactive ligands and their respective Fe(III) Co-ordination (A) Curcumin & Bidentate curcumin-Fe(III); (B) Quercetin & bidentate quercetin-Fe(III); (C) Gallic acid & bidentate gallic acid-Fe(III); (D) Tris bidentate curcumin-quercetin-gallic acid-Fe(III).

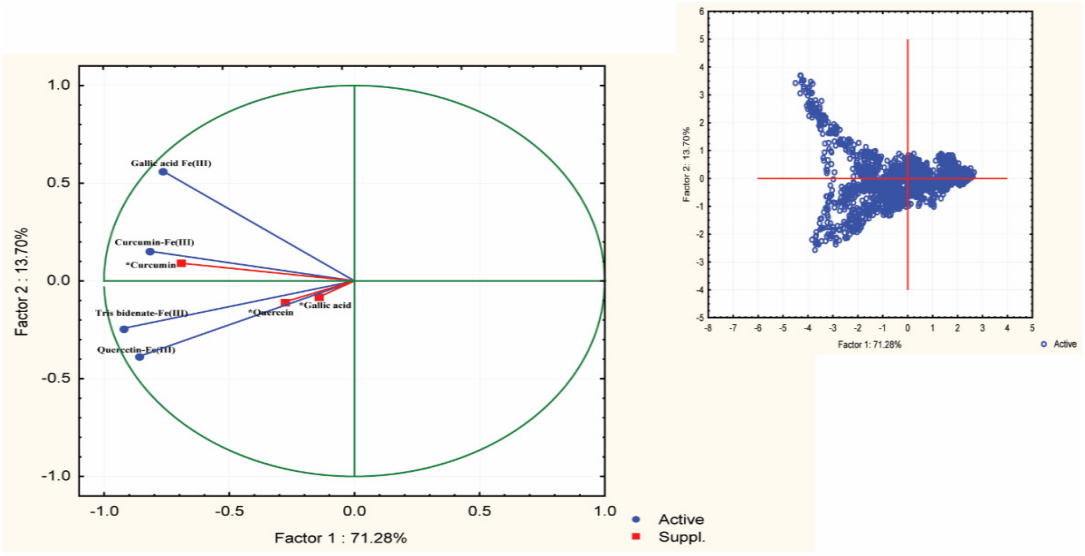
Gallic acid Fe(III)
Curcumin-Fe(III)
*Curcumin
Tris bidenate-Fe(III)
*Quercein
*Gallic acid
Quercetin-Fe(III)
Factor 2 : 13.70%
Factor 1 : 71.28%
Active
Suppl.
Factor 2: 13.70%
Factor 1: 71.28%
Active

(A)

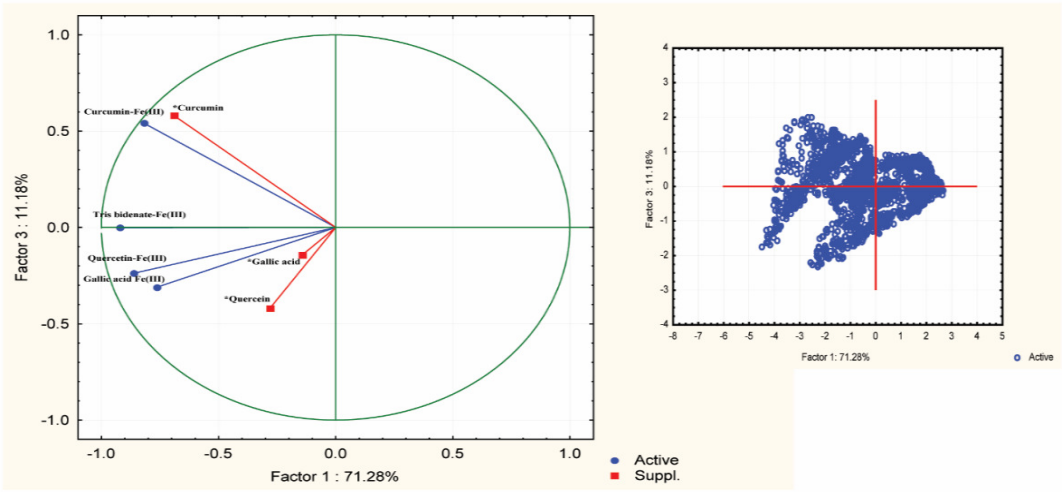
Curcumin-Fe(III)
*Curcumin
Tris bidenate-Fe(III)
Quercetin-Fe(III)
Gallic acid Fe(III)
*Gallic acid
*Quercein
Factor 3 : 11.18%
Factor 1 : 71.28%
Active
Suppl.
Factor 3: 11.18%
Factor 1: 71.28%
Active

(B)

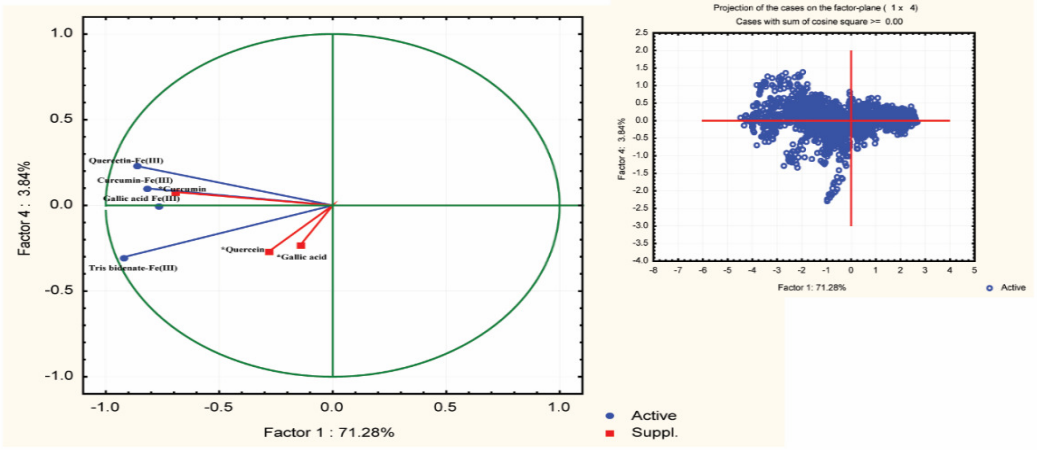
Quercetin-Fe(III)
Curcumin-Fe(III)
*Curcumin
Gallic acid Fe(III)
*Quercein
*Gallic acid
Tris bidenate-Fe(III)
Factor 4 : 3.84%
Factor 1 : 71.28%
Active
Suppl.
Projection of the cases on the factor-plane (1 x 4)
Cases with sum of cosine square >= 0.00
Factor 4: 3.84%
Factor 1: 71.28%
Active

(C)

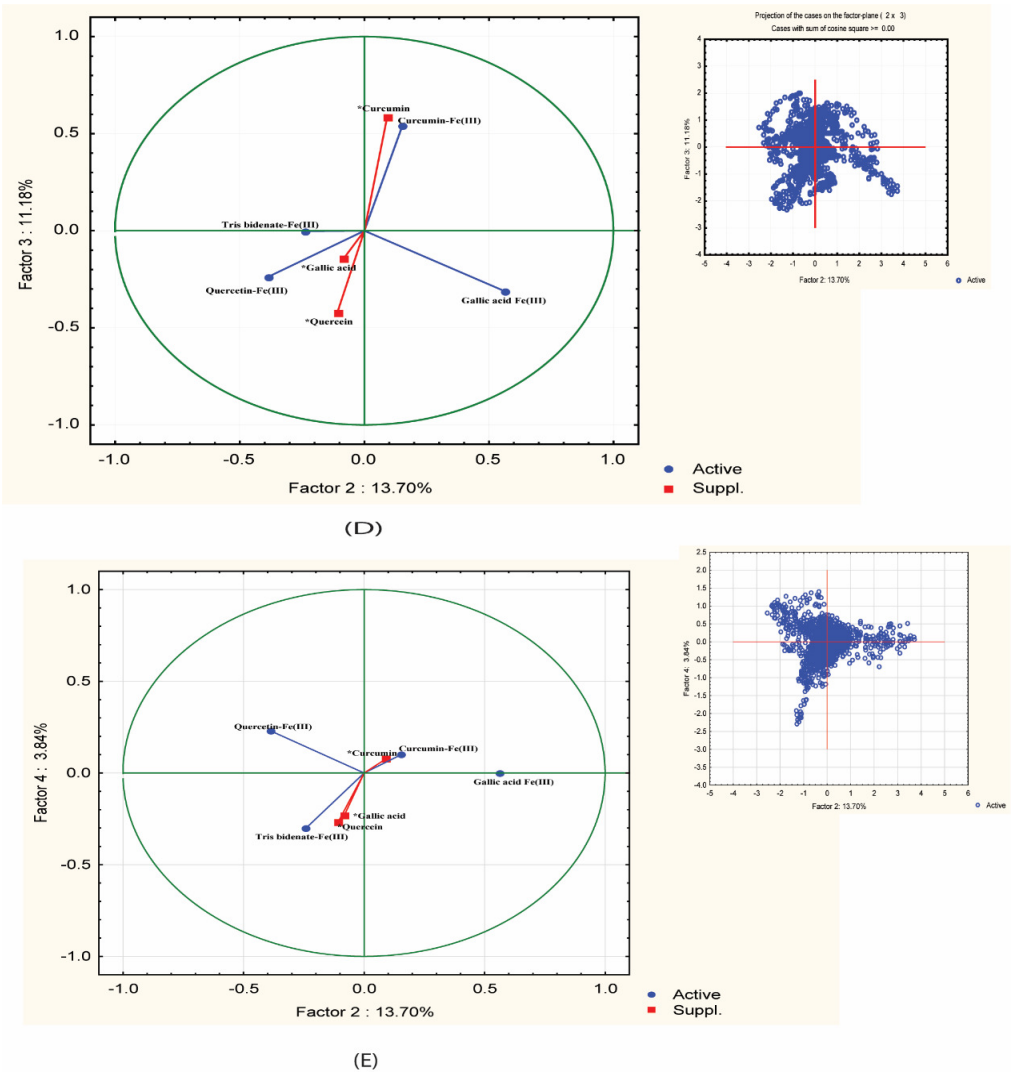

Fig. 4(A-D): PCA analysis for bioactive ligand(s) [termed as supplementary] & their respective Fe(III) coordination complex [termed as active] (A) loading plot of factor 2 v/s factor 1(B) loading plot of factor 3 v/s factor 1 (C) loading plot of factor 4 v/s factor 1 (D) loading plot of factor 3 v/s factor 2 (E) loading plot of factor 4 v/s factor 2.

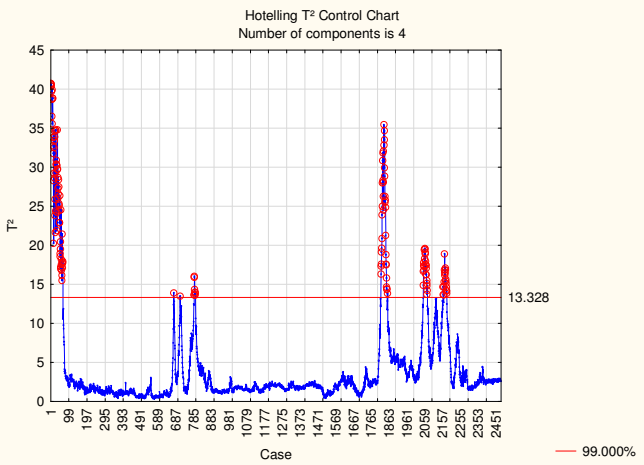

(A)

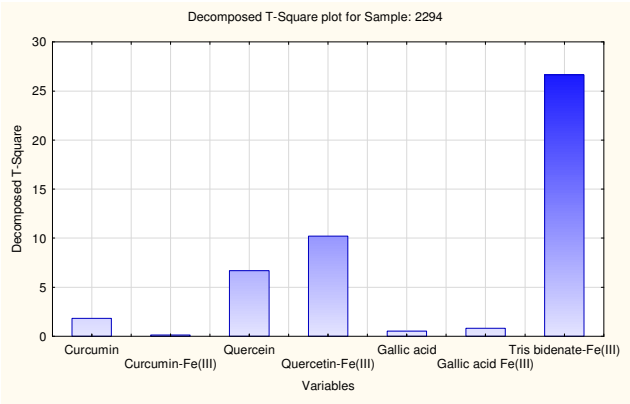

(B)

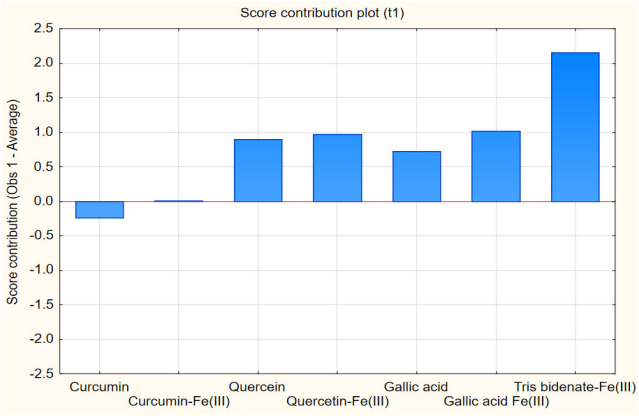

(C)

Fig. 5 (A, B): Monitoring charts for PCA integrate Raman spectroscopy bioactive ligands and their respective coordination complexes (A) Hotelling T^2 analysis chart (B) Decomposed T^2 Plot (C) Score contribution plot.

Table 1: Directionality analysis of SEM image slices indicting Gaussian spline direction (°), dispersion (°), amount and goodness of fit.

Slice	Direction (°)	Dispersion (°)	Amount	Goodness
Curcumin	-2.96	24.32	0.68	0.80
Curcumin-Fe(III)	59.83	31.39	0.58	0.65
Quercetin	-49.97	26.53	0.57	0.56
Quercetin-Fe(III)	-14.37	25.84	0.66	0.71
Gallic acid	0.05	1.05	0.09	0.61
Gallic acid-Fe(III)	81.40	17.09	0.40	0.92
Tris-bidenate [Curcumin-quercetin- -gallic acid-Fe(III)].	0.06	0.82	0.02	0.39

Table 2: DSC profile of bioactive ligands and their respective Fe(III) co-ordination complexes.

	Endotherm-1				Endotherm-2				Endotherm-3				Endotherm-4				
Ligands / co-ordination complex	T_{onset} (^{0}C)	Peak (^{0}C)	T_{endset} (^{0}C)	ΔH (Jg^{-1})	T_{onset} (^{0}C)	Peak (^{0}C)	T_{endset} (^{0}C)	ΔH (Jg^{-1})	T_{onset} (^{0}C)	Peak (^{0}C)	T_{endset} (^{0}C)	ΔH (Jg^{-1})	T_{onset} (^{0}C)	Peak (^{0}C)	T_{endset} (^{0}C)	ΔH (Jg^{-1})	T_{onset} (^{0}C)
Curcumin	174.92	177.58	180.71	-119.3	-	-	-	-	-		-	-	-		-	-	-
Curcumin-Fe(III)	51.92	59.32	82.04	-18.07	144.63	159.78	165.84	-17.23	168.51	181.3	208.93	-6.1	258.92	261.96	297.72	-45.86	-
Quercetin	249.81	252.99	259.48	-5.31	-	-	-	-	-		-	-	-		-	-	-
Quercetin-Fe(III)	180.12*	178.42	186.51*	-	251.42	258.36	266.86	-2.61	286.66	295.1	303.37	-78.34	-		-	-	-
Gallic acid	93.75	114.74	123.71	-307	254.02	254.56	259.31	-162.18	-		-	-	-		-	-	-
Gallic acid-Fe(III)	50.6	52	56.87	-3.04	142*	144.7	178.31*	-	177.27	178.31	179.59	-0.0062	219.72	232.53	241.08	-194.95	-
Tris-bidentate	50.56	82.94	83.08	-211.63	136.22	142.07	150.33	-11.59	174.6	174.92	175.37	-0.0052	207.35	212.31	230.93	-16.75	267.42

*Glass transition temperature.

Table 3: Loading of active and supplementary variables corresponds for four principal components along with correlation matrix, eigenvalue & % total variance.

Variables	Factor 1	Factor 2	Factor 3	Factor 4
Curcumin-Fe(III)	-0.820250	0.152680	0.542224	0.099353
Quercetin-Fe(III)	-0.861312	-0.386310	-0.237805	0.228812
Gallic acid Fe(III)	-0.765873	0.562692	-0.311151	-0.000018
Tris bidenate-Fe(III)	-0.921932	-0.242376	-0.001771	-0.302147
*Curcumin	-0.692506	0.091059	0.582434	0.077845
*Quercetin	-0.280845	-0.108090	-0.419720	-0.268413
*Gallic acid	-0.142588	-0.082559	-0.142351	-0.231648
Eigen value	2.851190	0.547915	0.447376	0.153519
% Total variance	71.28%	13.70%	11.18%	3.84%

*Supplementary variable